Military Technical College
Kobry El-Kobbah,
Cairo, Egypt

6th International Conference
on
Chemical & Environmental
Engineering
29 -31 May, 2012.

ENMA-4

EFFECT OF PACKING PARAMETERS ON THE COMBUSTION BEHAVIOR OF AP BASED COMPOSITE SOLID PROPELLANT

A.Maraden*, Hosam E.Mostafa*, S.Hasanien*

Abstract

Ammonium Perchlorate (AP) is frequently employed in the form of bimodal mixtures as an oxidizer in composite propellant formulations. Hydroxyl Terminated Polybutadience (HTPB) is also frequently used as a prepolymeric fuel binder in these propellants. The combustion behavior of this heterogenous mixture depends on both packing density and specific surface area of the oxidizing particles. One of the reliable packing models has been selected and employed for calculating the packing parameters of many of monomodal and bimodal mixtures. A one dimentional lab scale vibrator has been employed for measuring the packing density. A remarkable agreement has been detected between the calculated and the experimentally obtained values. Packing factor of about 0.64 and 0.82 has been recorded for the monomodal and the bimodal mixtures respectively. One of the efficient two dimentional combustion models has been selected and employed for predicting the flame structure and the regression surface for some selected propellant formulations. The results prevailed the important role of the packing parameters regarding both the flame structure and the regression surface

Keywords

Composite Propellant, Packing density, AP packing, AP/HTPB, Combustion behavior.

* Egyptian Armed Forces

1. Introduction

Ammonium Perchlorate (AP) / Hydroxyl Terminated Poly-Butadiene, (HTPB) composite rocket propellant is widely used in a variety of rocket systems ranging from small tactical missiles to the large boosters that propel the space shuttle into orbit. The burning behavior and flame structure of an AP/HTPB composite propellant are influenced by many factors including the chamber pressure, AP particle size and mass fraction [1]. Three facts are realized for a typical AP/HTPB composite propellant under consideration. First, the mass loading of AP is much higher than that of HTPB. Second, AP monopropellant is highly reactive and can sustain exothermic reactions without the presence of any fuel binder. Third, the size of AP particles plays a decisive role in dictating the burning behavior of the composite propellant [2, 3]. AP degradation is thus regarded as the controlling factor in the combustion of AP/HTPB composite propellant. To describe the complex gas phase flame structure, many assumptions about the components (fuel + oxidizer) in the system have been made. That is weather these components are mixed before combustion (premixed flame), or whether the two components must first diffuse together before the combustion can take place (diffusion flame). The following models have been adopted to furnish the baseline for the complex flame structure.
The basic idea for the burning of the rocket propellant is further illustrated in 1998 by Jeppson [4], as shown in Fig.1.

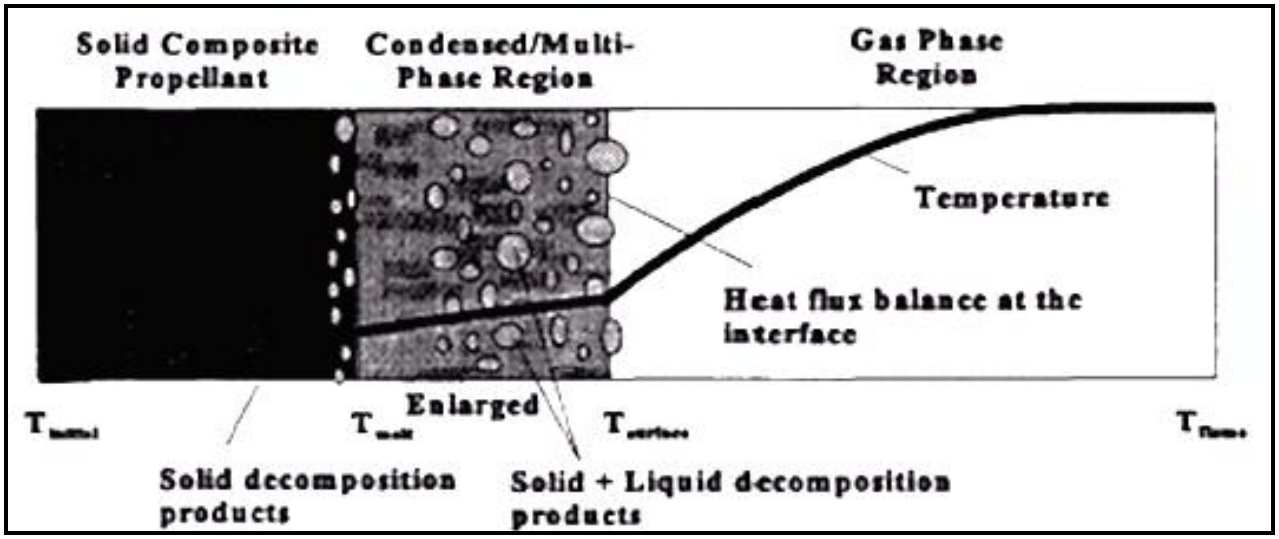

Figure 1. Composite Solid Propellant Combustion Layers

Three separate flames can be identified in the gas phase [5]; primary flame between the decomposition products of the binder and the oxidizer, premixed oxidizer flame and final diffusion flame between the products of the other two flames, fig. 2.

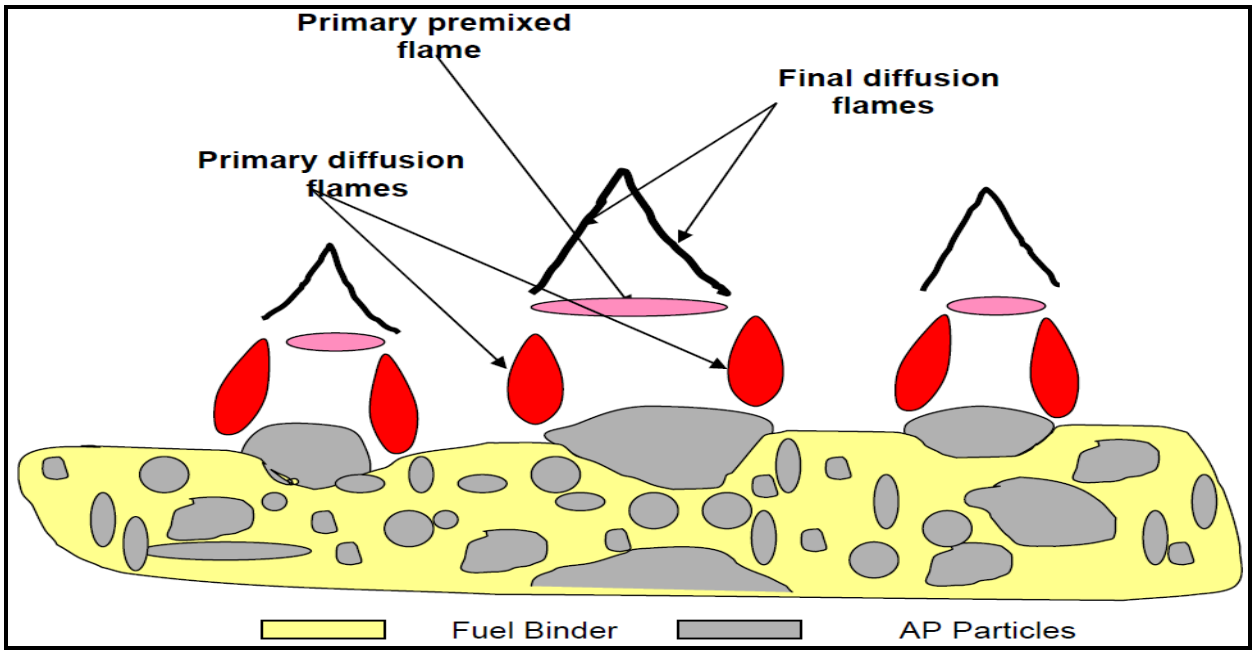

Figure 2. Flame Structure of AP/Binder Composed Propellant

The combustion of AP/HTPB can be improved by increasing the AP mass content but we cannot do this for technological considerations, so we may improve the combustion of AP/HTPB by improving the packing density of AP using the most perfect particle size distribution of two (may be more)different particle sizes[6]. The industry constructs propellants by mixing a selection of AP cuts in suitable proportions. Each cut is characterized by a nominal size, 200, 50, 20 μm, etc., but there is a wide range of sizes within each cut. It is instructive to examine some true cuts.

McGeary, in 1961 [7] reported a brief description of some experiments on the packing of steel shot. Bimodal packing was investigated in which spheres of diameter 0.124 in. are packed with smaller spheres. The packing volume is defined as the volume of the particles plus the interstitial volume. The packing fraction ρ which is defined as the volume fraction of the fine particles. When the particle volume fraction is either 0 or 100%, the packing is said to be monomodal and the packing fraction is approximately 0.625. Fig 4 shows the McGeary's data for the packing fraction.

Few decades ago, several theoretical studies on the combustion field of the burning of the heterogeneous propellant have been conducted. These researches are divided into two main categories. The first one is concentrated on the gas phase modeling without consideration for the condensed phase process. The second one is studied the condensed phase reaction as the most important factor.

Recently, few studies have been employed the complex coupling between the solid-phase and gas-phase process, by solving the full Navier-Stokes in the gas-phase simultaneously with the energy one in the solid phase During the 1960's, 70s and into 80s, several models have been proposed to describe the combustion of composite propellants. In general these models have been somewhat successful in correlating experimental data, but are not sufficiently accurate, or complete to predict burning rate behaviour. Only the work by Hermance in 1966, [8] considers the combustion problems over a broad range of pressure. Of course, like other models assumptions are made to convert the unsteady 3D process to a steady 1D model. The

principal mechanisms which Hermance put into this framework were a dominant AP-binder interfacial surface reaction, and a single premixed flame sheet in the gas.
In this work however, an unrealistics description of the propellant surface was assumed and the heterogeneous reaction was assumed to occur only between the oxidizer crystals and the binder. One of the most ambitious and famous model for the complex flame structure which furnishes the baseline for this review is proposed by Beckstead, Derr, and Price. Several improvements to BDP model of steady-state burning have been conducted. Lee [9] presented a modified picture for the flame structure for AP-Binder-AP sandwich as in Fig.3. This sketch show the principles of the combustion zone, in which the oxidizer-fuel flames consists of a leading-Edge Flame (LEF) that stands in the mixing region of the oxidizer and fuel vapors, and a diffusion flame that trails from the LEF up to a point where the fuel vapor is all consumed. The LEF is a region of very high heat release as compared to the rest of the diffusion flames and contributes most of the heat transfer back of the propellant surface. This edge occurs because the diffusion flame cannot extend all the way to the surface, the temperature there being too low. Most of the recent studies have been used the Lee model as a baseline for their computations [10,11].
Most of the recent studies [12] assumed that the diffusion flame in BDP model can be described by a Burke-Schumann flame sheet [13], thereby discarding the importance role played by the leading edge of this flame. Jepsson in 1998 [4] show that, as illustrated in Fig.3 the fact that differing sizes of the AP grains within the binder require different assumptions about the gas phase flame.

Combustion modeling for multimodal composite propellants requires both premixed and diffusion flame theory. Fine AP sizes within the binder can be modeled as a premixed flame. Increasingly coarse AP sizes, however, approach an AP monopropellant flame, while mid-range AP sizes require diffusion flame calculations.

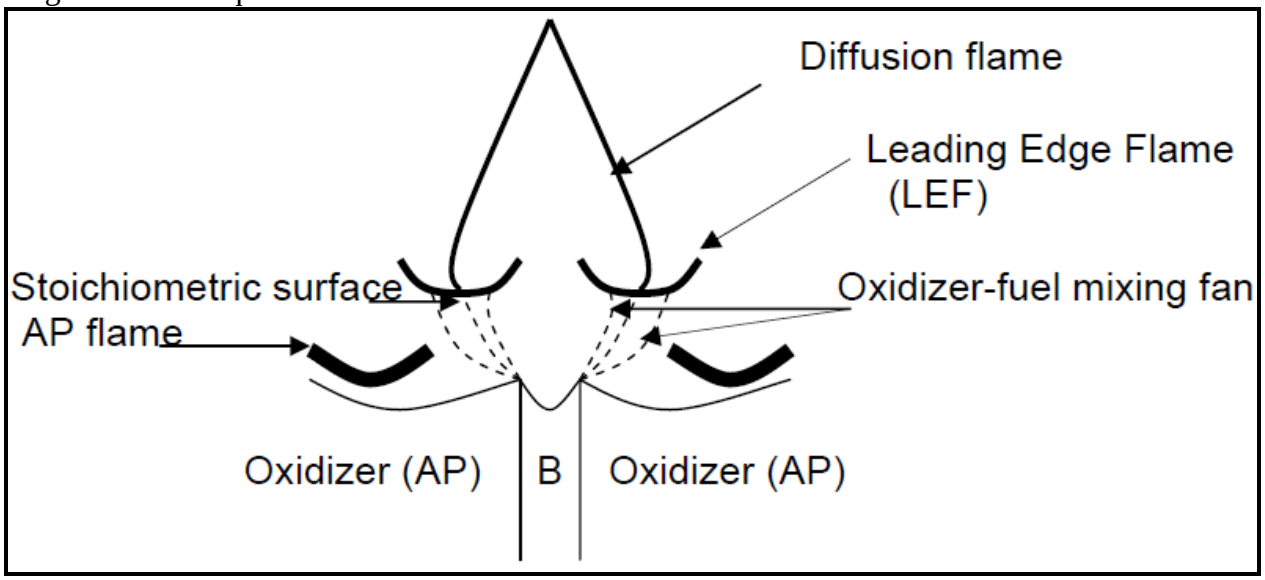

Figure 3. Flame Structure of AP/Binder Composite Propellant by Beckstead, Derr, and Price (BDP)

Recently Hegab in 2001 [15,16] developed a mathematical model that described the unsteady burning of a rocket propellant by simultaneously solving the combustion field in the gas-phase and the thermal field in the solid-phase, with appropriate jump conditions across the gas/solid interface (combustion surface). Propagation of the unsteady non-planar

regressing surface is described by using a level-set formulation which gives rise to a Hamilton–Jacobi equation [15].

In the present paper a complete numerical strategy account the primary flame between the decomposition products of the binder and the oxidizer (AP), the primary diffusion flame from the oxidizer (AP), different properties (density, conductivity) of the AP and binder, an unsteady non-planer regression surface by utilizing Hegab model. These ingredients are applied to the problem of Periodic 2D packing disks with different AP grain sizes distributed in a HTPB fuel-binder.

2. Theoretical Treatment of Packing

The packing density would be governed by the particle size distribution of the particles. Consider the simplest case of a binary mixture (two distinct sizes). When a small amount of smaller particles is added to the larger particles, the smaller particles would fill the voids between the larger particles and thereby increase the packing density (filling effect) fig.5. Higher packing fractions are achieved for bimodal packs and the greater the disparity in sizes, the greater the packing fraction. In all cases, the maximum occurs at approximately 30% fine, 70% coarse. The largest packing fraction is 0.8594.

A mathematical models for the 2D random packing strategies have developed by Kochevets [17], Knott [18], and Buckmaster [19] in order to numerically construct models of heterogeneous rocket propellants. Their packing algorithms are based on the integration of the random packing approach and the collision theory that has been described in a number of papers by Lubachevsky and his Colleagues in 1990,1991 [20]. These models deal with 2D combustion field supported by a disk pack propellant, in which full coupling between the gas phase, the condensed phase, and the retreating nonplanar propellant surface was accounted.

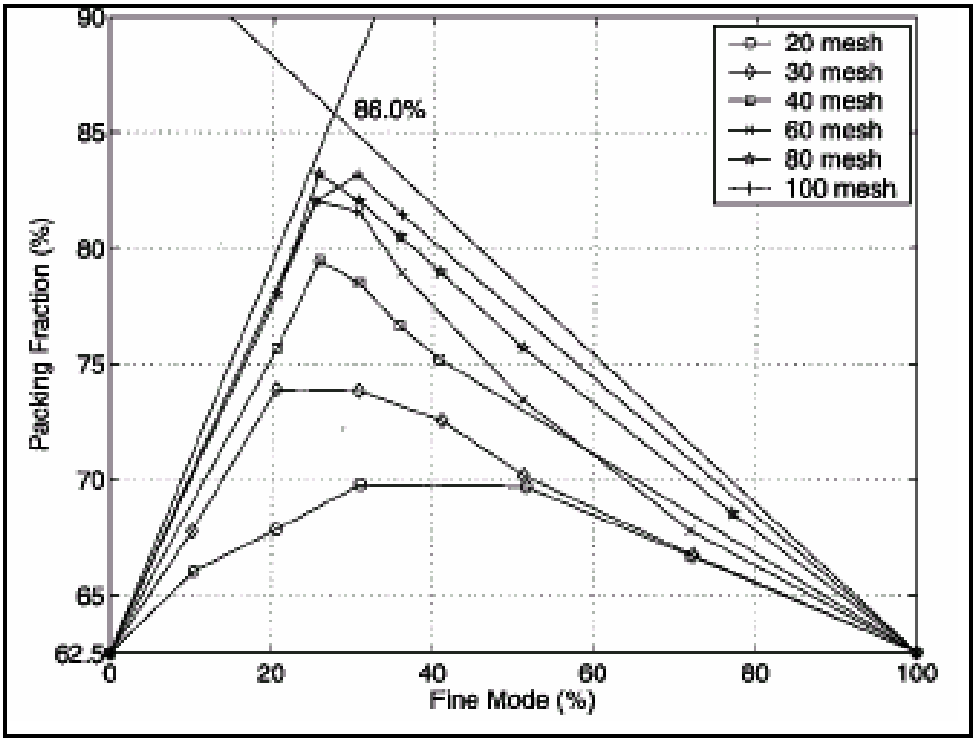

Figure 4. McGeary's Data for Packing Fraction

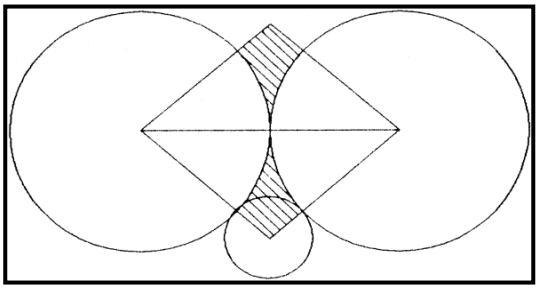

Figure 5. Felling Effect for Increasing Packing Density

Recently, in 2007, Hegab [21,22] describes a large number of periodic 2D disk pack models by assuming that the particles of the AP are 2D disks and distributing them in a random fashion and applied to monomodal, bimodal, and multimodal disc packs. The disk packs that used in the current study are a large grey AP (375 micron) distributed with smaller sizes of AP grains.

3. Experimental Determination of AP Packing Fraction

An experimental verification carried out using the vibration device for the AP particles. The setup is able to vibrate in one direction with different amplitudes and frequencies. This operation simulates the process of composite propellant manufacturing by adding the needed amount of AP through three equal amounts with shaking and mixing for thirty minutes for each adding. The raw material selected for investigation were ammonium perchlorate powder (NH_4ClO_4) with mean particle diameter of 10 – 500 µm, with density 1.95 g/cm^3, Molecular weight 117.49 and Melting point, 315 ^oC. The experimental packing was carried out by drying AP powder in vacuum oven for 24 hours at 80 °C, Adjusting the conditions of lab environment to be humidity < 30% and temperature < 30 °C, AP powder Sieved by sieving analysis for 20 min. the Raw material used is Ammonium perchlorate (NH_4ClO_4) of density 1.95 g/cm^3 and Molecular weight of 117.49 and Melting point 315 ^oC. After sieving we get six different particle sizes of mean particle size 375 & 187.5 & 107.5 & 76.5 & 47.5 & 10 microns which are allowed in lab scale from 32µm to 1mm. The tubes of volume 13.5 ml, fig 6, are cleaned using distilled water, dried in an oven at 60 °C and cooled down to room temperature. The tubes was then fixed in the vibration device, fig 7, and the particles were poured down gently into the tube to form the initial packing (particle size 187.5 & 107.5 & 76.5 & 47.5 & 10 with the large one 375). The packing was then vibrated under a given condition for a period of time and stopped and the packing density was re-determined. The packing density is defined by the volume of the AP divided by the volume of the tube.

Packing fraction = AP volume / Tube volume

4. Theoretical Treatment for AP Composite Propellant Combustion

The BDP model identifies three kinds of flames, but it has long been argued that the "primary diffusion flame," in which AP and binder gases react, is not important. The two survivors are the AP decomposition flame and the final diffusion flame in which the AP decomposition products react with binder gases; these two flames are part of the two-dimensional model discussed here. The two-step kinetics that include the AP decomposition flame and the final diffusion flame is examined in order to achieve a good understanding of the unsteady burning of periodic 2D disk pack propellant with complete coupling between the solid and gas phases. Thus

$$AP(X) \xleftrightarrow{R_1} decomposition\ products(Z)$$

$$\beta Z + Binder(Y) \xleftrightarrow{R_2} final\ products$$

R_1 and R_2 are assumed to have the forms;

$$R_1 = B_1\, P\, X \exp(-E_1/R_u T) \quad (1)$$

And $$R_2 = B_2\, P^{ng}\, Y\, Z \exp(-E_2/R_u T) \quad (2)$$

Where B's are the exponential prefatory, E's are the activation energy in the gas phase, P is the pressure, R_u is the universal gas constant, and (T, X, Y and Z) are the temperature, oxidizer, fuel and the decomposition products respectively. The output of the packing model is treated to be an input for the combustion model.

Table 1: Thermophysical properties of the gas, AP, and Binder

Parameter	value	Parameter	value
Gas Phase		Q_{AP} (kcal/kg)	+100.86
ρ_g (kg/m^3)	8		
λg (W/m.K)	0.209	A_{AP} (cm/s)	9.82x10^4
c_p (kcal/kg.K)	0.3	ρ_B (kg/m^3)	920
Q_{g1} (kcal/kg)	675	λ_B (W/m.K)	0.184
Q_{g2} (kcal/kg)	3127	c_B (kcal/kg.K)	0.3
E_g (kcal/mole)	31.2	Q_B (kcal/kg)	- 47.8
R_u (kcal/kmole.K)	1.985		
Solid Phase		A_B (cm/s)	4.96x10^3
E_{AP} (kcal/mole)	22	T_0 (K)	300
E_B (kcal/mole)	15	$T_{ref,g} = Q_g/c_p$ (K)	2700
ρ_{AP} (kg/m^3)	1950	P_0 (atm)	1
λ_{AP} (W/m.K)	0.628	m (kg/m^2.s)	18
c_{AP} (kcal/kg.K)	0.3	$T_{ref,AP,B}$ (K)	860

5. Results and Discussion

Theoretical Results for Packing

Each AP particle size was treated alone by the packing algorithm then each particle size was treated with the largest particle size as shown in fig.5. S is the size ratio of small / large.

Experimental Results for Packing

After sieving we get six different particle sizes, and then packed to give five mixtures. Table 1 shows the obtained different particle sizes. As the size ratio increases, the form of the theoretical curve of packing density of a perfect real mixture plotted against the proportion of large particles, shows a flat region and a shift of its maximum to lower value of this proportion. The packing density, however, is lower when the size ratio of coarse particles to fine particles decreases.

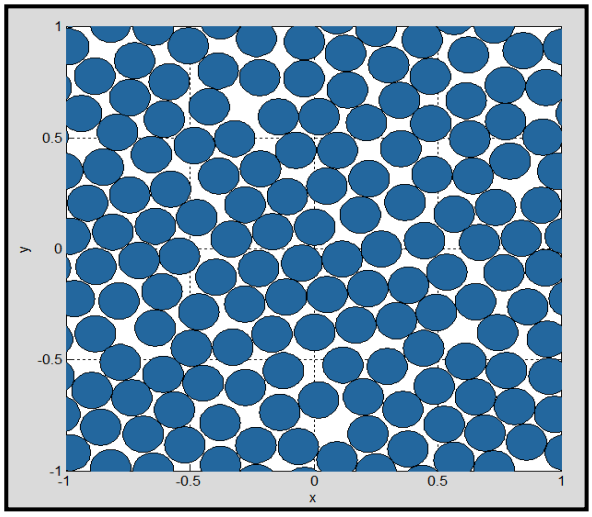

Mono particle size packing

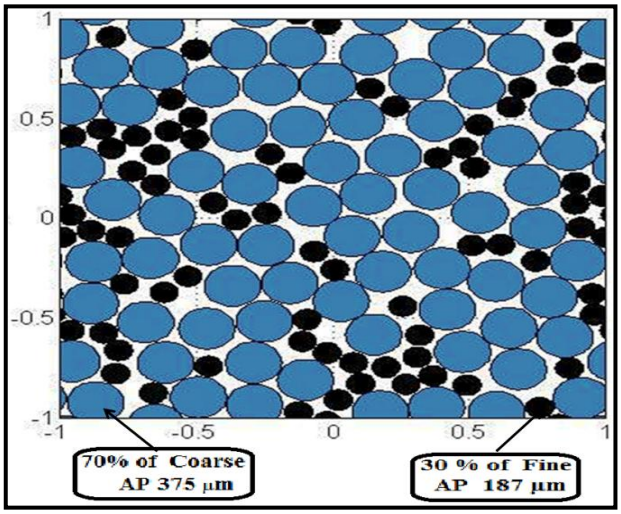

Binary mixture packing S = 0.5

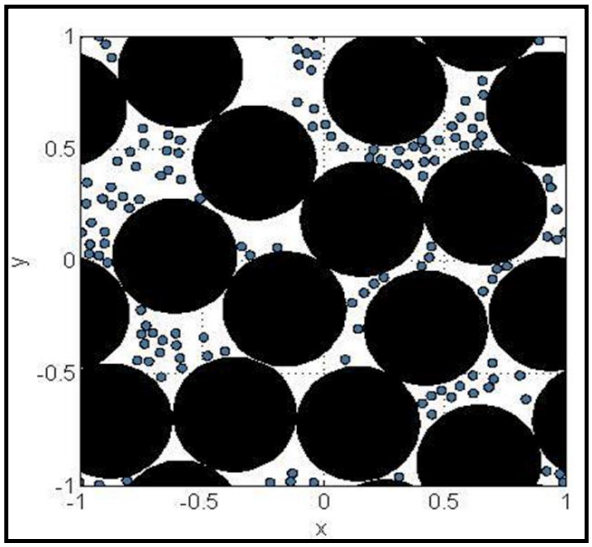

Binary mixture packing S = 0.027

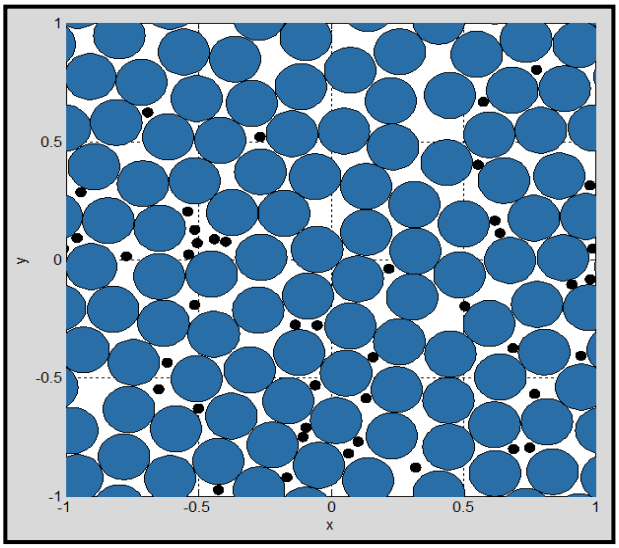

Binary mixture packing S = 0.287

Figure 6. Theoretical Packing Results for Different Particle Sizes

A high maximum packing density is directly dependent upon the particle size distribution. Many studies have demonstrated the importance of the particle size distribution to obtain dense packing. For a two component mixture of coarse and fine particles, the ideal packing density is predicted to be about 0.82 at 70% coarse and 30% fine. When the particle volume fraction is 0 or 100%, the packing is monomodal and the packing fraction is approximately 0.64. Higher packing fractions are achieved for bimodal packs and the greater the disparity in sizes, the greater the packing fraction. In all cases, the maximum occurs at approximately

30% fine, 70% coarse. The largest packing fraction implied by this data is about 0.82.the results were represented in table 2 and Fig 9.

Table 1 Different Particle Sizes and Corresponding Mesh Numbers

Mesh	µm	Average	
		mesh	µm
60-35	250-500	45	375
120-60	125-250	90	187.5
170-120	90-125	145	107.5
230-170	63-90	200	76.5
400-230	32-63	315	47.5
1250	7-11	1250	10

Comparing the real experimental of AP's with the sphere shots by McGeary, [15] is found to be qualitatively similar Packing Density = Mass of AP / (Density of AP × Volume of tube)

$$PD = \frac{M(APc)}{\rho(APc) * V(tube)}$$

Where the density of AP is 1.95 g/cm^3 and the Volume of tube is13.5 ml

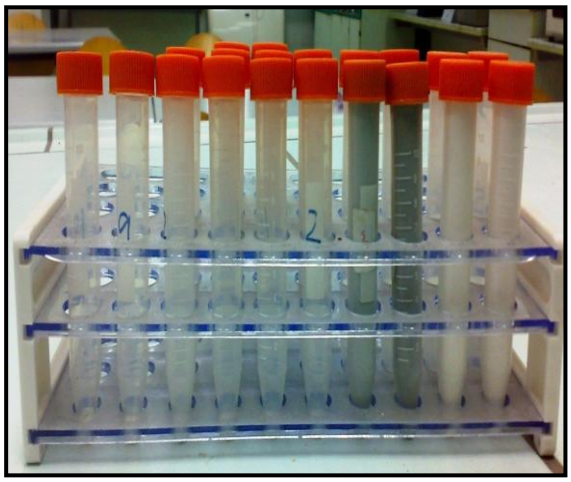

Figure 7. Tubes Used for Measuring Packing Density

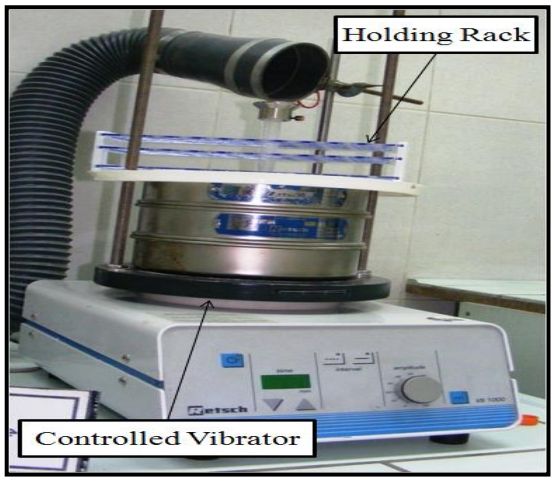

Figure 8. Vibrator Used for Packing Operation

Theoretical Results for AP composite propellant combustion

The understanding of the complex combustion structure of the 2D disk pack of AP/HTPB propellant, as a simple model to the heterogeneous solid rocket propellant, is studied in details for three different bimodal packing models to show the effect of the AP grain sizes and distribution with the fuel binder on the combustion process, the burning rate, and the flame structure. The gas phase of these three models is the constant density model where the density is set equal to constant. Initially, the solution starts for the three models from a flat surface Then the solution is advanced simultaneously in the solid/gas phases, with moving interface with appropriate jump conditions.

Table (2) Packing Fractions for the Packed Samples

Codes		Empty Tube Mass (g)	Filled Tube Mass (g)	AP Mass Filled-Empty (g)	AP Volume AP Mass/1.95 (cm^3)	Packing Fraction AP vol/Tube vol
	X	5.3163	22.4498	17.1335	8.7864	0.6461
	B	5.4058	22.4364	17.0306	8.7336	0.6422
	N	5.5133	22.4615	16.9482	8.6914	0.6391
	Y	5.6074	22.5683	16.9609	8.6979	0.6396
	Z	5.4951	22.4439	16.9488	8.6917	0.6391
	A	5.5148	22.4303	16.9155	8.6746	0.6378
X (%) +B (%)	**X9B1**	5.3163	22.7657	17.4494	8.9484	0.6628
	X7B3	5.4058	23.2696	17.8638	9.1609	**0.6786**
	X5B5	5.5133	23.2575	17.7442	9.0996	0.6740
	X3B7	5.6074	23.3999	17.7925	9.1244	0.6759
	X2B8	5.4951	22.8824	17.3873	8.9166	0.6605
	X1B9	5.5148	22.6457	17.1309	8.7851	0.6507
X (%) +N (%)	**X9N1**	5.5116	23.5486	18.0370	9.2497	0.6852
	X7N3	5.3882	24.2588	18.8706	9.6772	**0.7168**
	X5N5	5.5125	23.6744	18.1619	9.3138	0.6899
	X3N7	5.3841	23.2512	17.8671	9.1626	0.6787
	X2N8	5.5269	22.9839	17.4570	8.9523	0.6631
	X1N9	5.4047	22.6704	17.2657	8.8542	0.6559
X (%) +Y (%)	**X9Y1**	5.4705	24.0491	18.5786	9.5275	0.7057
	X7Y3	5.5079	25.7292	20.2213	10.3699	**0.7681**
	X5Y5	5.5079	25.2209	19.7130	10.1092	0.7488
	X3Y7	5.6287	24.4082	18.7795	9.6305	0.7134
	X2Y8	5.6075	23.6435	18.0360	9.2492	0.6851
	X1Y9	5.5298	23.0442	17.5144	8.9817	0.6653
X (%) +Z (%)	**X9Z1**	5.4047	24.3298	18.9251	9.7052	0.7189
	X7Z3	5.5116	26.3145	20.8029	10.6682	**0.7902**
	X5Z5	5.3882	25.8727	20.4845	10.5049	0.7781
	X3Z7	5.6074	24.1227	18.5153	9.4950	0.7033
	X2Z8	5.3841	23.2627	17.8786	9.1685	0.6791
	X1Z9	5.5269	22.7441	17.2172	8.8293	0.6540
X (%) +A (%)	**X9A1**	5.4705	24.5172	19.0467	9.7675	0.7235
	X7A3	5.5079	27.0859	21.5780	11.0656	**0.8197**
	X5A5	5.5079	26.0158	20.5079	10.5169	0.7790
	X3A7	5.4951	24.5205	19.0254	9.7566	0.7227
	X2A8	5.6075	23.7554	18.1479	9.3066	0.6894
	X1A9	5.5298	22.9152	17.3854	8.9156	0.6604

Where the code name matches the mesh numbers

Code	X	B	N	Y	Z	A
(µm)	250-500	125-250	90-125	63-90	32-63	7-11
Mesh Number	45	80	140	200	300	1250

For the bimodal disk pack defined in models (I). (II), and (III) showed in fig 10, where a large grey AP (375 µm) distributed with smaller sizes of AP grains (187 micron each) (model I) and large grey AP (375 µm) distributed with smaller sizes of AP grains (47 micron each) (model II) and large grey AP (375 µm) distributed with smaller sizes of AP grains (107micron each) (model III) by 70% of large particles with 30% of smaller particles.
The upper portion represents the gas phase and the lower one refers to the solid phase. The circles regions in the latter represent the AP grains (gray), while the powder around the circles represents the fuel-binder HTPB. The combustion surface shape through the solid phase show that the surface is initially flat and then as the solution is advanced, the combustion surface retreats in an unsteady fashion and the morphology of the combustion surface reflects the AP size and distributions.

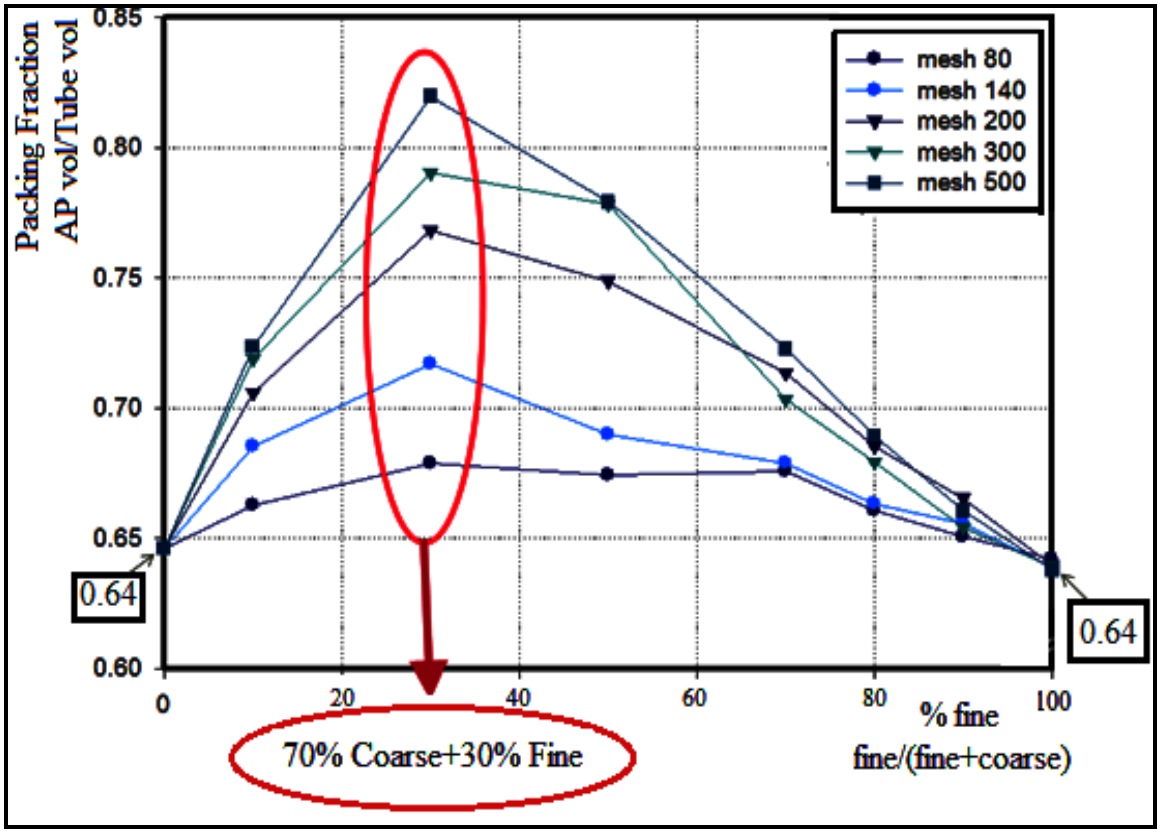

Figure 9. Relation Between Packing Fraction and Percentage of Fine Powder.

The differences in shapes of the reaction rates contours with time illustrate the behavior of the burning rate at the propellant surface and are used to reconstruct the corresponding flame structures and identify the parts of the flame structure that dominate the 2D disk pack burning rate and the surface heat flux. It is noted that, when a significant portion of the surface consists a large AP grains as in the model (I), the local regression is slower than that where mixing of small AP grains with binder occurs as in model (II) and (III) at later times.

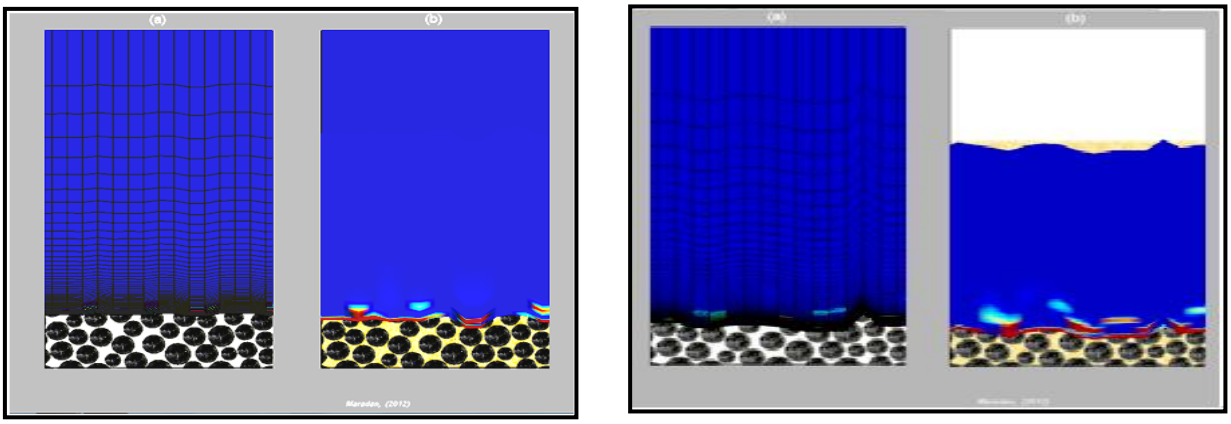

(model I)

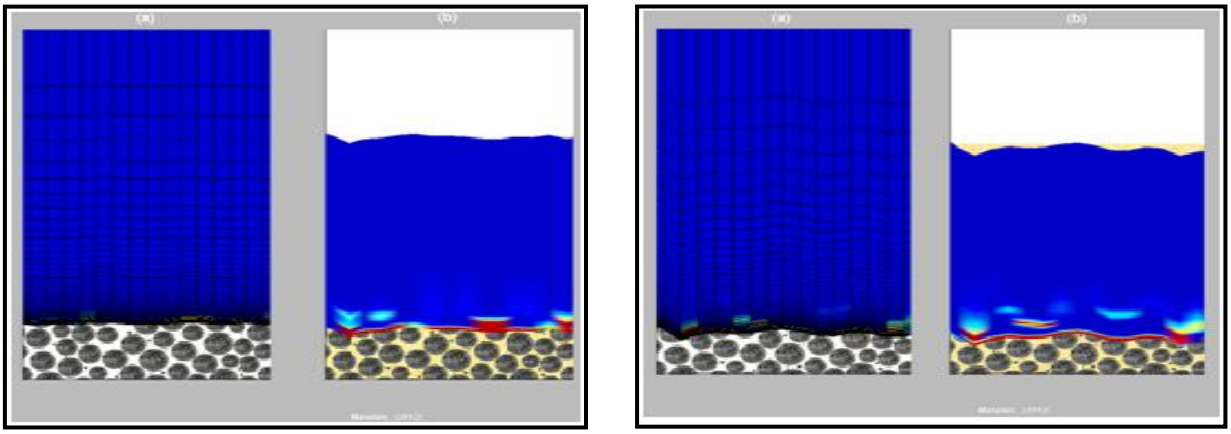

(model II)

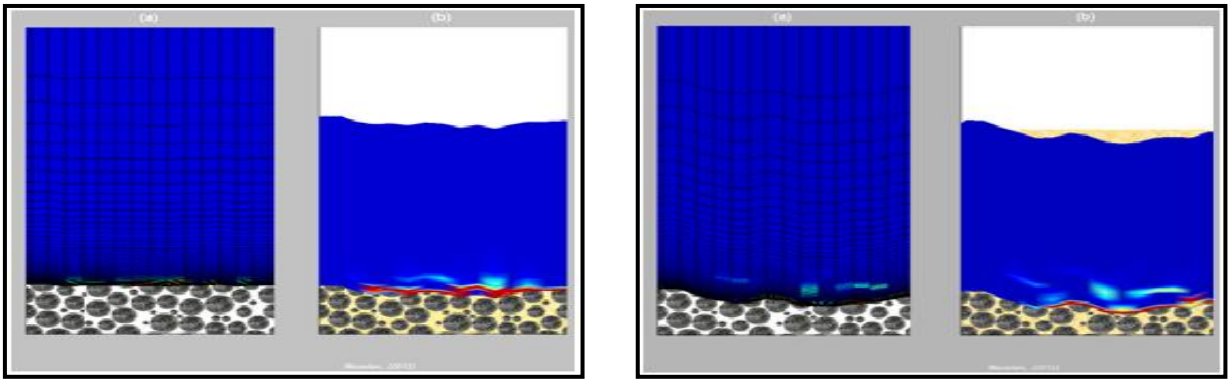

(model III)

Figure 10. Reaction Rate Contours for the Selected Models.

In additions these figures show two kinds of flames. The first ones are the AP decomposition flames. These flames represent the horizontal flame structures over the combustion surface and lie adjacent to the small and large AP grains. As time advanced, these horizontal shapes converted to curved ones to reflect the burned portions of the AP grains. The second flames are the diffusion flames that generated at the interface between the AP grains and the fuel-

binder HTPB. These flames represent the vertical flame structure at the interfaces points between the fuel and oxidizer. As time advanced, these diffusion flames take a different shapes in the gas phase and may meet each other in a very nice way to form another flames away from the combustion surface.fig 11showes the temperature gradient in the solid phase of composite solid propellant, fig 12 shows the total area burned with time and fig 13 shows the total mass burned with time.

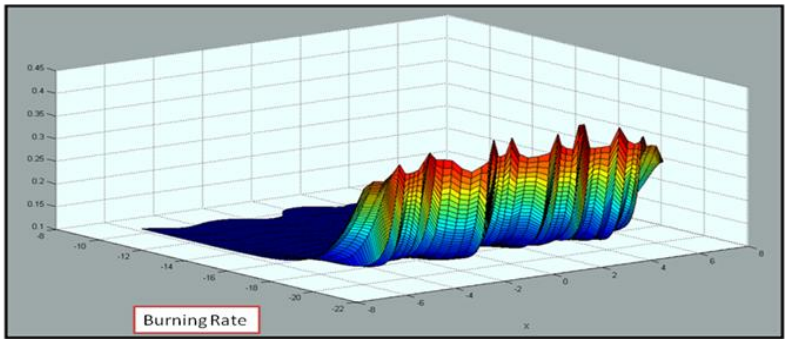

Figure 11. Temperature Gradient in the Solid Phase

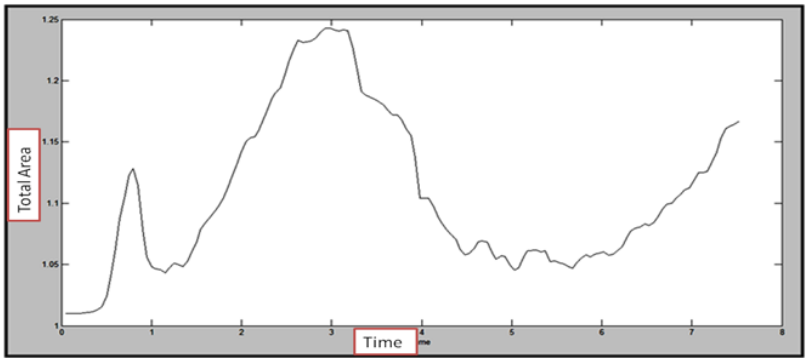

Figure 12. Total Area Burned With Time

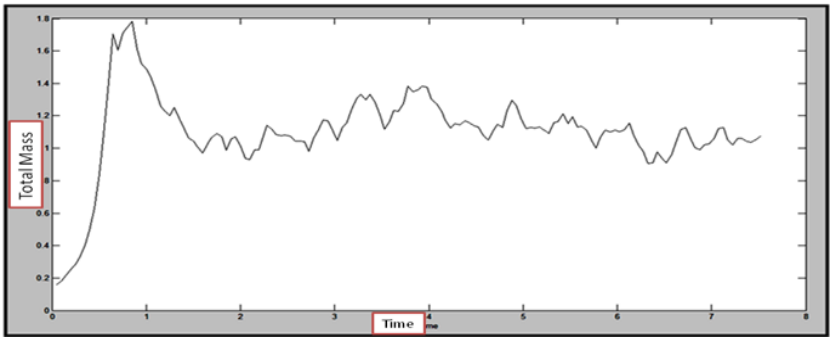

Figure 13. Total Mass Burned With Time

6. Conclusion

Here, random packing for bimodal (2 different grain sizes) is discussed also experimental investigation is performed. The mass loading of AP is typically much larger than HTPB (more than three times). The AP size and the size distribution have a great effect on the burning rate. The packing density of monosize spheres can reach 0.74, if the spheres are carefully arranged in an ordered pattern. In reality, however, the spheres tend to be randomly arranged with a packing density of only 0.60 when un-vibrated or 0.64 when vibrated, the packing density of monosize particles is governed by two factors: the packing condition and

particle shape. The combustion of AP/HTPB can be improved by increasing the AP mass content. The ideal packing density is predicted to be about 0.82 at 70% coarse and 30% fine. For binary mixtures the size ratio has great effect on packing density, as size ratio increase the packing fraction decrease, for size ratio equal unity the mixture would be monosized. By applying the results obtained from the packing model to combustion model after experimental verification for the most useful size ratio and packing fraction, 2D calculations to the combustion of heterogeneous solid propellant, accounting for the gas phase physics, the solid phase physics and an unsteady non-planar description of the regressing propellant surface is used. Three different random packing disc models for the AP particles imbedded in a matrix of fuel-binder are used as a base of our combustion code. These models have different AP grain sizes and distribution within the fuel binder. The effect of AP grain sizes and distribution with the fuel-binder HTPB on the shape of the combustion surface and the flame structure was studied by presenting three different random discs packing for bimodal models. It is clearly seen that the AP grain size has a great effect not only on the combustion surface and the generated flame structure but also on the gas/solid phases and interface temperature, the equivalent ratios, and surface mass flux as well. It is clearly seen that the large AP particles act as a resistance in the way of the combustion process and, in turn, slow down the burning of the combustion surface comparing with the mixture of small particles imbedded in HTPB powder.

References

[1] W. Cai and V. Yang, "A Model of AP/HTPB Composite Propellant Combustion", AIAA Paper 2000-0311, 38th Aerospace Science Meeting (2000).

[2] Kochevets, S., Buckmaster, J., and Jackson, T. L., "Random propellant packs and the flames they support", 36th AIAA/ASME/SAE/ASEE Joint Propulsion Conference. AIAA Paper 2000-3461, 2000.

[3] Hegab, A.M. "Random Packing of Bimodal and Multimodal Heterogeneous Propellant", in press, 2007.

[4] Jeppson, M. B., Beckstead, M. W., and Jing, Q., "A Kinetic Model for the Premixed Combustion of a Fine AP/HTPB Composite Propellant," 36th Aerospace Sciences and Exhibit, AIAA-98-0447, Jan. 12-15, 1998, Reno, NV.

[5] M.W. Beckstead, R.L. Derr, and C.F. Price, "A Model of Composite Solid- Propellant Combustion Based on Multiple Flames", AIAA Journal, 8(12):2200- 2207, (1970).

[6] Hegab, A.M. (2007), "Effect of ammonium perchlorate grain size on combustion of a selected composite solid propellant"; The 12th International Conference on Aerospace Science & Aviation Technology, ASAT-12, May 2007, Cairo, Egypt.

[7] McGeary, R. K., "Mechanical Packing of Spherical Particles," Journal of the American Ceramic Society, Vol. 44, No. 10, 1961, pp. 513–522.

[8] Hermance, C.E. "A Model of Composite Propellant Combustion Including Surface Heterogeneity and Heat Generation", AIAA Journal, Vol.4 PP 1629-1637, (1960).

[9] Lee, S., Price, E. and Sigman, R., "Effect of Multidimensional Flamelets in Composite Propellant Combustion", ", Journal of Propulsion and Power, Vol.10(6), PP 761-768, (1994).

[10] Jackson, T.L., Buckmaster, J. and Hoeflinger, J. "Three-Dimensional Flames Supported by Heterogeneous Propellants", JANNAF Paper, JANNAF CS/PSHS/APS Joint Meeting, Cocoa Beach, FL. October (1999).

[11] Jackson, T.L., Buckmaster, J. and Hegab, A.M. " Periodic Propellant Flames and Fluid-Mechanical Effects", Journal Propulsion and Power Vol. 17, Number 2, Pages 371-379, (2001).

[12] Hegab, A., Jackson, T., Buckmaster, J., and Stewart, S., "Nonsteady Burning of Periodic Sandwich Propellant with Complete Coupling between the Solid and Gas Phases" Combustion and Flame, Vol. 125(1/2), PP 1055-1070, (2001).

[13] Jia, X. and R. W. Bilger, "The Burke- Schumann Diffusion Flame with Zero Net Flux Boundary Conditions," Combustion Science and Technology, Vol. 99, 371-376, 1994.

[14] Hegab, A.M. (2003), "Modeling of Microscale Solid Propellant Combustion"; The Tenth International Conference on Aerospace Science & Aviation Technology, ASAT-10, May 13-15, 2003, Cairo, Egypt.

[15] Kochevets, S., Buckmaster, J., and Jackson, T., and Hegab, A.,"Random Packs and their Use in Modeling Heterogeneous Solid Propellant Combustion", Journal of Propulsion & Power Vol.17 No.4, pp. 883-891, July-Aug. 2001.

[16] Kochevets, S., Buckmaster, J., and Jackson, T. L., "Random propellant packs and the flames they support", 36th AIAA/ASME/SAE/ASEE Joint Propulsion Conference. AIAA Paper 2000-3461, 2000.

[17] Knott, G. M., Jackson, T. L., and Buckmaster, J., "The Random Packing of Heterogeneous Propellants," AIAA Journal, Vol. 39, No. 4, pp. 678– 686.

[18] Buckmaster J., Jackson T., Hegab A., Kochevets S., Ulrich M. "Randomly Packed Heterogeneous Propellants and the Flame They Support" AIAA paper 2001-0337, 39th. Aerospace Science Meeting, Reno, NV, 2001.

[19] Lubachevsky, B. D., and Stillinger, F. H., "Geometric Properties of Random Disk Packings," *Journal of Statistical Physics*, Vol. 60, Nos. 5/6,pp. 561–583, 1990.

[20] Hegab, A.M. (2003), "Combustion Modeling of Micro-Structure Solid Propellant"; Engineering Research Journal ERJ, Minufiya University, Vol. 26, No.3, July 2003.